PARAMETRIC 1-D MODELING STUDY OF A 5-STROKE SPARK-IGNITION ENGINE CONCEPT FOR INCREASING ENGINE THERMAL EFFICIENCY

A Thesis
SUBMITTED TO THE FACULTY OF THE GRADUATE SCHOOL
OF THE UNIVERSITY OF MINNESOTA
BY

Alex Melin

IN PARTIAL FULFILLMENT OF THE REQUIREMENTS
FOR THE DEGREE OF
MASTER OF SCIENCE

William F. Northrop
(Faculty Adviser)

July 2016

Acknowledgements

I would like to start by thanking Prof. William F. Northrop for stopping me in the hallway and providing me with the opportunity to attend graduate school. Without that conversation I would probably never have given graduate school a though.

I would like to thank Prof. David B. Kittelson for his support throughout my entire academic career at the University of Minnesota.

I would also like to recognize the help that I have received from Mark Claywell, and Donald Horkheimer throughout my academic career. They both played a major role in providing me the necessary guidance to obtain the knowledge base required for this project.

Lastly I would like to thank Kurt Amplatz, for without his idea and generous donation for without this none of this research would have been possible.

Dedication

This thesis is dedicated to my parents Duane and Kristina Melin. From a young age they encouraged my creativity, curiosity, and love of taking things apart. Without their support I would never have attended the University of Minnesota let alone be graduating with my Master's Degree.

I would also like to dedicate this thesis to my uncle John Segelstrom. Uncle John was more than just an uncle, he was my buddy, my golf and fishing partner, my second father. I could go on for days about him, but in the end it will always come back to him being my "Uncle John" and I will be his "Big Al".

Abstract

In recent years, there has been growing interest in alternative cycles to the standard 4-stroke Otto engine for improving efficiency and lowering emissions of spark-ignition engines. One proposed concept is the 5-stroke engine, which uses two cylinders, a combustion cylinder and an expansion cylinder with a transfer port between them. Excess pressure in the combustion cylinder can be further expanded by using a second expansion cylinder to harness additional work. The expansion cylinder runs on a two-stroke cycle, allowing the use of two combustion cylinders to one expansion cylinder in a three-cylinder configuration to increase efficiency. Previous work has investigated the performance of prototype 5-stroke engines compared to 1-D modeling results; none have conducted a thorough study on the interactions of various design parameters. In this paper, we explore the results of a 1-D parametric modeling study to examine the effect of various parameters such as bore, stroke, valve lift profiles, and compression ratio on engine brake thermal efficiencies of a three cylinder 5-stroke engine. Over the range of values examined our work indicates that an expansion cylinder bore to stoke ratio of 1.4 and expansion ratio 17.5 produces maximum brake thermal efficiency. The intake, transfer, and exhaust lift profiles have a strong effect on brake thermal efficiency with valve opening and closing points playing a key role. Additionally, reducing the offset between the combustion and expansion cylinder improves the timing of the transfer process leading to improved brake thermal efficiency. Lastly, the transfer volume between the combustion and expansion cylinder has minimal effect on the brake thermal efficiency.

Table of Contents

List of Tables

List of Figures

1 Introduction

Ever more stringent environmental regulations continue to motivate the need to improve efficiency and reduce emissions of internal combustion engines. In August of 2012 the Environmental Protection Agency (EPA) and Department of Transportation's National Highway Traffic Safety Administration (NHTSA) issued a regulatory announcement outlining the fuel economy and greenhouse gas standards for 2017-2025 [1]. This announcement outlines the reduction in CO_2 emissions and sets the miles per gallon (mpg) for automotive manufactures entire fleet. The announced regulation calls for combined CO_2 emissions to be 163 grams/mile, which corresponds to a Corporate Average Fuel Economy (CAFÉ) of 54.5 mpg by model year 2025.

In an effort to achieve the mandated fuel economy targets, extensive research is being dedicated to various strategies with much of the effort being focused on two high level areas; reducing pumping losses at part load operation without sacrificing peak performance, and increasing the amount of work extracted from the power cycle for a given fuel input. In order to apply these strategies in production engines, various concepts are being implemented including the use of charging systems (like a turbo or supercharger), smaller displacement engines, cylinder deactivation, electric hybridization, or alternative thermodynamic cycles.

The use of a charging system with a smaller displacement engine is a growing trend among automotive manufactures. Charging allows an engine to maintain peak performance while reducing the pumping losses at part load. During high load conditions the charge system is used to increase the peak power of the engine by increasing the

density of the air entering the cylinder. At part load the output of the charge system is reduced which allows the throttle valve to stay open wider. By allowing the throttle valve to stay open the pumping losses of the engine are reduced leading to improved part load efficiency during normal cruising conditions. Due to the limit on the amount of charging that is possible before knock occurs and the losses associated with both turbo- and super-chargers this approach has a limited level of improvement.

Cylinder deactivation is another method used to reduce pumping losses during part load operation. During high load conditions all of the cylinders are active allowing for peak power to be produced by the engine. During part load conditions, instead of closing the throttle to reduce power, cylinders are turned off (ie, deactivated). This is commonly done by keeping both the intake and exhaust valves closed which results in the deactivated cylinder acting like a pneumatic spring. As cylinders are deactivated the other cylinders have to produce more work, which means that the throttle has to be open more leading to a reduction in pumping losses. This method however does not remove the friction losses as the deactivated cylinder is still moving. Due to the limit on the amount of work that can be produced by a cylinder, and that friction losses still exist in the deactivated cylinder, the amount of efficiency improvement achievable by this strategy is reduced.

Hybrid power systems used in automobiles come in two general forms, series, and parallel [2]. A series hybrid system consists of four major components, an IC engine, generator, battery, and electric motor. In a series hybrid system the IC engine drives a generator that provides energy to the battery where it can either be stored for use later or

provided to the electric motor to drive the wheels. A parallel hybrid system consists of just the IC engine, battery, and electric motor. In a parallel hybrid system, the IC engine can provide energy to both the wheels and the electric motor at the same time. This means that when the engine produces more power than required by the wheels the electric motor serves as a generator and charges the battery. Once the battery is charged, the IC engine can be turned off and the electric motor can drive the wheels. Alternatively, if more energy is required then what can be provided by the IC engine, the electric motor provides additional power to the wheels to meet the demand. The goal of the hybrid system is to improve efficiency by allowing the engine to operate at a steady state point where the engine has been optimized to operate. This allows for improved thermal efficiency and reduced emissions with the drawback being that hybrid systems increase the weight, cost, and control systems required to control energy delivery.

Alternative cycles are variations on the standard Otto Cycle, the ideal thermodynamic cycle used to represent the closed cylinder portion of spark ignition engine operation. These variations utilize numerous strategies to change the shape of the pressure versus volume (PV) diagram to try and increase the amount of usable work produced. To achieve this, parameters such as valve timing, compression ratio (CR), or expansion ratio (ER) are manipulated or the cycle is split or extended through the use of additional cylinders. Some examples of alternative cycles or split cycles are the Atkinson, or Miller cycle, Scudari concept, or Five-Stroke. These concepts will be discussed in greater detail in the following section.

1.1 Background

1.1.1 Otto Cycle

The standard SI engine cycle is referred to as the Otto Cycle after Dr. N.A. Otto. Dr. Otto originally patented a stationary engine that used what is now known as the Otto cycle in 1876 [3]. Over the past 100+ years many technological improvements have been made but the basic concept of the Otto Cycle has remained unchanged. To compare the performance of different cycles a pressure versus volume (PV) diagram is used. This can be generated using ideal air-standard cycle, simulation software, or measured data. Figure 1 shows a representative log-log PV diagram created using the ideal air-standard method. The ideal air-standard cycle uses air as working fluid and contains the following thermodynamic processes: adiabatic compression from 1-2 (compression stroke), constant volume heat addition from 2-3 (combustion), adiabatic expansion from point 3-4 (expansion stroke), and constant volume heat rejection from 4-1 (exhaust stroke). Typically, a log-log scale is used when examining PV diagrams to allow for straight lines for the expansion and compression stroke where the slope of the line is related to the ratio of specific heats for air which is used when calculating the adiabatic compression and expansion.

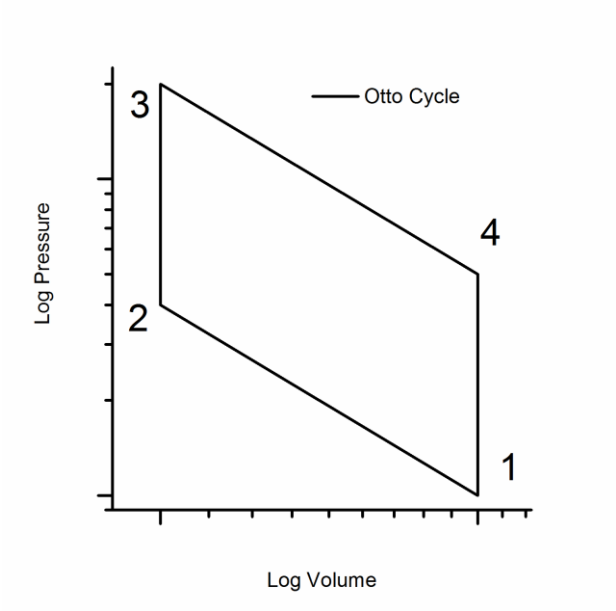

Figure 1: Representative log-log PV diagram of standard Otto Cycle

Over the years many have worked to improve the performance of a standard SI engine by increasing power output or improving efficiency. One common method for improving the efficiency and increasing the power output of an SI engine is increasing the CR. For a standard SI engine with equal compression and expansion strokes, CR and ER are equal and the thermal efficiency for an ideal cycle can be calculated using Equation 1 where r_v is the compression ratio and gamma is ratio of specific heats for the gas being used.

$$\eta_{Otto} = 1 - \frac{1}{r_v^{\gamma-1}}$$

Equation 1: Ideal Otto Cycle Thermal Efficiency

From Equation 1 it would appear that to improve the thermal efficiency of the Otto cycle one would just increase the CR. There is, however, a practical CR limit that can be

implemented before abnormal combustion occurs. One common form of abnormal combustion that limits practical spark ignition engine CR is knock, spontaneous ignition that occurs ahead of the flame front where small combustion events happen in the air fuel charge. Knocking occurs due to increased temperature and pressure conditions in the cylinder that pre-ignite the fuel, resulting in large pressure spikes. Since prolonged or severe knock will result in damage to the engine the CR has to be limit to avoid inducing knock. The maximum thermal efficiency achievable in a standard Otto cycle is largely determined by the knock limited CR.

While it is common practice to use CR when describing the ideal Otto Cycle efficiency, it is actually ER that has the greatest effect on actual thermal efficiency. Since the ER and CR are the same for the Otto Cycle, they are not separately specified in the classical thermodynamic analysis. This is not the case for split cycle concepts where CR and ER are purposely separated to increase thermal efficiency.

1.1.2 Split Cycle

As previous stated, split cycle concepts physically separate the ER from the CR. Research has focused on the efficacy of split cycle concepts to increase engine efficiency [4]–[7]. As mentioned previously, CR is limited by abnormal combustion. However, ER can be increased for a given CR thus increasing the amount of work done in the expansion stroke for a fixed amount of compression. Mallikarjuna et al. [5] found that using a late intake valve closing strategy to vary the ratio between CR and ER while keeping the CR constant resulted in a 3.3% increase in brake thermal efficiency for a CR of 8:1 and 7.96% increase with a CR of 7:1 when the ER is 1.5 times larger than the CR.

This is just one example of the various methods used to separate CR and ER that will be discussed in more detail in the following sections.

1.1.3 Miller Cycle

The Miller cycle was originally developed by Ralph Miller and was patented in 1957. The Miller cycle uses changes in valve timing to manipulate the effective CR to separate CR from ER [8]–[10]. By manipulating the intake valve closing (IVC) point, the effective CR is reduced when compared to the physical CR by allowing air to exit the cylinder resulting in a reduction of trapped mass inside the cylinder. This allows for the effective ER to be larger than the effective CR without modification of the crank train assembly. The ideal thermal efficiency for the Miller cycle can be calculated using Equation 2 and 3 where r_e is the ER, r_c is the CR, r_{ce} is the effective compression ratio, Q_{LVH} is the lower heating value of the fuel being used, and F is the fuel to air ratio.

$$\eta_{Miller} = 1 - \frac{\gamma r_e^{\gamma-1}(r_e - r_{ce}) + \theta r_{ce} + r_{ce}^{\gamma} - r_e^{\gamma}}{\theta r_c r_e^{\gamma-1}}$$

Equation 2: Ideal Miller Cycle Thermal Efficiency

$$\theta = \frac{Q_{LVH} F}{C_v T_1}\left(\frac{r_{ce} - 1}{r_{ce}}\right)$$

Equation 3: Miller Cycle Constant

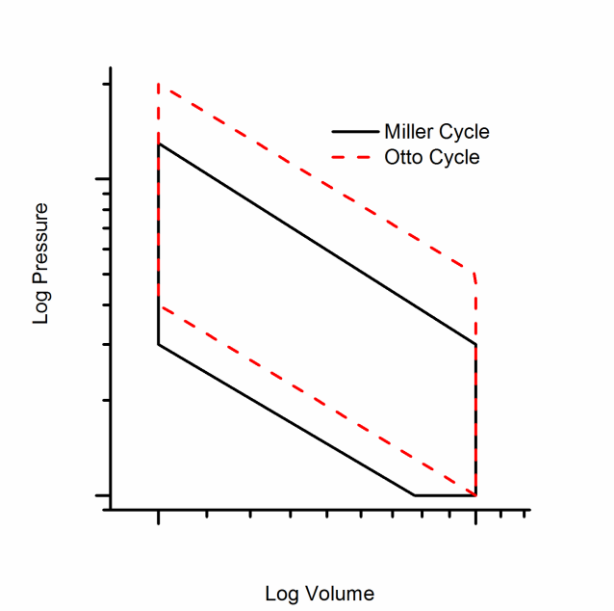

Figure 2: Representative Log-Log PV diagram of ideal Miller Cycle compared to ideal Otto Cycle

Figure 2 shows the P-V diagram for the ideal Miller Cycle compared to the ideal Otto Cycle. When comparing the two cycles visually, the area of the P-V diagram for the Otto Cycle is larger than that of the Miller Cycle. However, when the amount of heat input into each cycle is compared to the amount of heat rejected by each cycle it becomes clear that the Miller cycle has a higher thermal efficiency. The Miller Cycle improves efficiency by reducing the pumping work, the work performed during the exhaust and intake stroke, when compared to the Atkinson Cycle along with decreasing the CR with respect to the ER. It is important to note that and engine using valve timing to manipulate the CR and ER is known as a Miller Cycle engine, it is common practice to describe a cycle with early IVC as a Miller Cycle and late IVC as an Atkinson Cycle which will be discussed later.

The use of early IVC compared to late IVC is what leads to a reduction in pumping work compared to Atkinson Cycle. Wan et al. [11] investigated the use of the Miller cycle at part load operation, brake mean effective pressure of 2 bar, and found that by advancing the IVC point by 89˚ crank angle degrees (CAD) the effective ER increased from 8.9 to 11.6, while the effective CR remained constant resulting in a pumping work decreased of 0.62 bar and fuel consumption by 11%. Due to the reduction in valve lift associated with early IVC, the combustion duration is increased or misfire can occur due to the reduction of in-cylinder fluid motion. Vent et al. [12] found that using direct injection with a multiple injection strategy allowed for increased turbulence to be generated near the spark plug, stabilizing the initial flame kernel formation and thus reducing misfire. França et al. [13] investigated the use of fully variable valve train (FVVT) systems to further control the difference between the CR and ER. Since the use of electro-hydraulic valve actuating systems or cam-in-cam systems are becoming more feasible, the effective CR can be controlled in real time without the use of a throttle. This allows the power output of the engine to be reduced at part load while reducing the pumping losses, and keeps the compression ratio below the knock limit at high load resulting in improved efficiency. By using variable IVC to control load the indicated thermal efficiency increased by ~5.5% when compared to a standard Otto Cycle operating at 25% of peak load.

1.1.4 Atkinson Cycle

James Atkinson first patented the Atkinson Cycle in 1882. The original Atkinson Cycle separates the CR and ER by using a compression stroke that is physically shorter

than the expansion stroke [14]–[19]. To do this, the standard crankshaft in the engine is either augmented with another shaft that drives a coupler linkage to change the piston motion or a ring and planet gear system is attached to the crankshaft. For the original Atkinson Cycle, the ideal thermal efficiency can be calculated using Equation 4 where r_e is the ER and r_c is the CR. Equation 4 it is based on the assumption that the gases in the cylinder are fully expanded to either ambient or inlet pressure.

$$\eta_{Atkinson} = 1 - \frac{\gamma(r_e - r_c)}{r_e^{\gamma} - r_c^{\gamma}}$$

Equation 4: Ideal Atkinson Cycle Thermal Efficiency

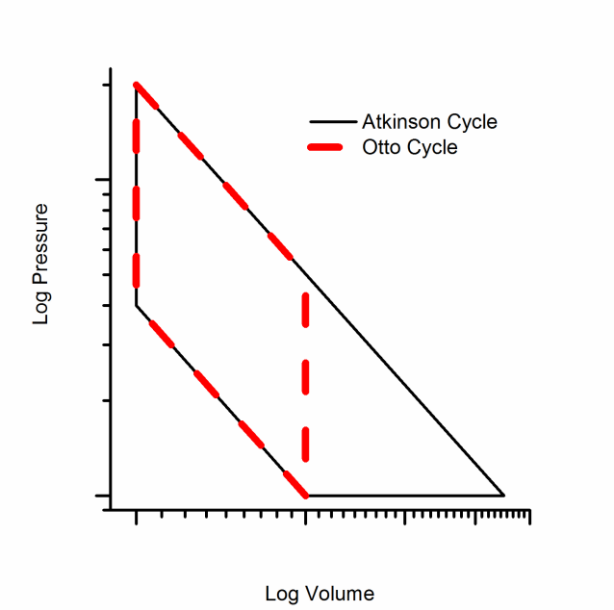

Figure 3: Representative Log-Log PV diagram of ideal Atkinson Cycle compared to ideal Otto Cycle

Figure 3 compares the original ideal Atkinson Cycle P-V diagram to that of the ideal Otto Cycle. By visually comparing the two cycles, it is possible to see where

additional expansion work is performed in the Atkinson Cycle compared to that of the Otto Cycle. By expanding the exhaust gas to ambient pressure the amount of work produced is increased during the cycle for the same energy input.

While the Atkinson Cycle is still a popular split cycle concept, it has come to represent a slightly different cycle. The current industry definition of an Atkinson cycle is actually a Miller cycle that uses late IVC instead of crank modification. Wan et al. [11] showed that by implementing a late IVC strategy where IVC was delayed by 44.4˚ CAD (IVC at 90˚ CAD aBDC intake) at high load, 8 BMEP at 2500 RPM, the BSFC was decreased by 13.9 g/kWh or 5.7% reduction in fuel used. Miklanek et al. [20] found that an IVC of 105˚ CAD aBDC, operating at BMEP of 2 bar or 23% of full load, resulted in a 3.8% increase in thermal efficiency at 1700 RPM and was increased to 4.4% by pre heating the intake charge.

By increasing the intake temperature charge to 120˚ C, the in-cylinder charge temperature at the start of ignition is closer to that of a standard Otto Cycle, which results in increased combustion efficiency when compared non-heated mixture. Pumping work is also reduced slightly with a heated mixture due to density reduction. Taylor et al. [21] investigated the use of a cam in cam design to vary valve timing and duration and found a part load reduction in BSFC of 17 g/kWh at 1000 RPM and 4 bar BMEP compared to the base line and a full load BSFC reduction of 4 g/kWh at 2500 RPM and 10 bar BMEP. The part load reduction is the result of reduced pumping work by delayed IVC. The full load reduction is the result of the engine being allowed to operate at max brake torque (MBT) spark advance when compared to the base line configuration. Typically, the spark

timing is retarded at full load to mitigate knock; however, by reducing the effective compression ratio, the spark can be advanced leading to improved fuel efficiency.

1.1.5 Scuderi Concept

The Scuderi engine is a split cycle concept that utilizes two pistons to complete the four-stroke cycle and was first patented by Carmelo Scuderi in 2003 [22]. By using two cylinders, the CR and ER can be completely separated with the first smaller cylinder (compressor cylinder), performing the intake and compression parts of the cyle while the second larger cylinder (expander cylinder), performs the combustion, expansion, and exhaust. The air is passed to the expander cylinder through a high passage air passage where fuel can be injected or it can be added directly into the expander cylinder. Due to the high turbulence created during the transfer process, the air-fuel mixing process and combustion event time are decreased reducing the time for knock to occur. Phillips et al. [23] found that an initial Scuderi engine had a minimum BSFC of 340 g/kWh when operating at 1200 RPM and a BMEP of 4.2 bar when operating under stoichiometric conditions. Branyon et al. [24] investigated the effects of downsizing the compressor cylinder and adding a turbocharger on a Scuderi engine. They found that 1500 RPM and a BMEP of 4.2 bar the BSFC was 320 g/kWh and by implementing a late IVC strategy to control load the BSFC was further reduced to 300 g/kWh.

1.1.6 Five-Stroke

The 5-stroke engine was initially patented by Lennox G. Newman in 2004 and, similar to the Scuderi concept, uses two cylinders [25]. The 5-stroke concept however

uses the additional cylinder to preform additional expansion work with the standard 4-strokes occurring in the first cylinder. The working details of the 5-stroke cycle will be covered in detail in section 2.1.

Previous work on the 5-stroke concept is limited. Ailloud et al. [26] showed that a 5-stroke engine for use as a range extending engine in a hybrid system fitted with a smart waste-gate concept achieved a peak BSFC of 226.4 g/kW-h resulting and a global efficiency of 36.1%. The smart waste-gate uses variable exhaust valve timing and only one of the two exhaust valves to allow exhaust gases to go to the turbo, which allows for reduced exhaust gas back-pressure.

The goal of this thesis is to provide a better understanding of the 5-stroke engine cycle by investigating basic thermodynamic application, the effect of the most important parameters to optimize a 5-stroke engine, and the practical use of a 5-stroke engine for on road use. The sparse previous published information on the 5-stroke concept has shown that the technology is viable for efficiency improvement but does not give a thorough description of the complex nature of gas dynamics coupled with the thermodynamic processes [26]. This work used a 1-D computer model to study the effect of key geometric and operating parameters on 5-stroke engine efficiency.

2 5-Stroke Concept

2.1 5-Stroke Cycle Description

The 5-stroke engine relies on the use of two cylinders, a combustion cylinder which performs the primary intake and combustion processes and an expansion cylinder

which allows for over-expansion. A transfer port resides between the two cylinders to allow exhaust products to flow from the compression cylinder to the expansion cylinder. Practical 5-stroke engines use two combustion cylinders sharing one expansion cylinder. This is optimal because the expansion cylinder runs on a 2-stroke cycle while the combustion cylinders operate on a 4-stroke cycle.

Figure 1 provides a stroke-by-stroke illustration of the 5-stroke engine. During the intake process in the combustion cylinder (stroke 1) the expansion cylinder is exhausting (stroke 5). Then compression occurs in the combustion cylinder (stroke 2) while the expansion cylinder is expanding the gases from the other combustion cylinder not shown in the figure (stroke 4). As the combustion cylinder is expanding (stroke 3) the expansion cylinder is exhausting again (stroke 5). Finally, the transfer port is opened and the exhaust is blown down from the combustion cylinder to the expansion cylinder (stroke 4) creating the over-expansion responsible for increased engine efficiency.

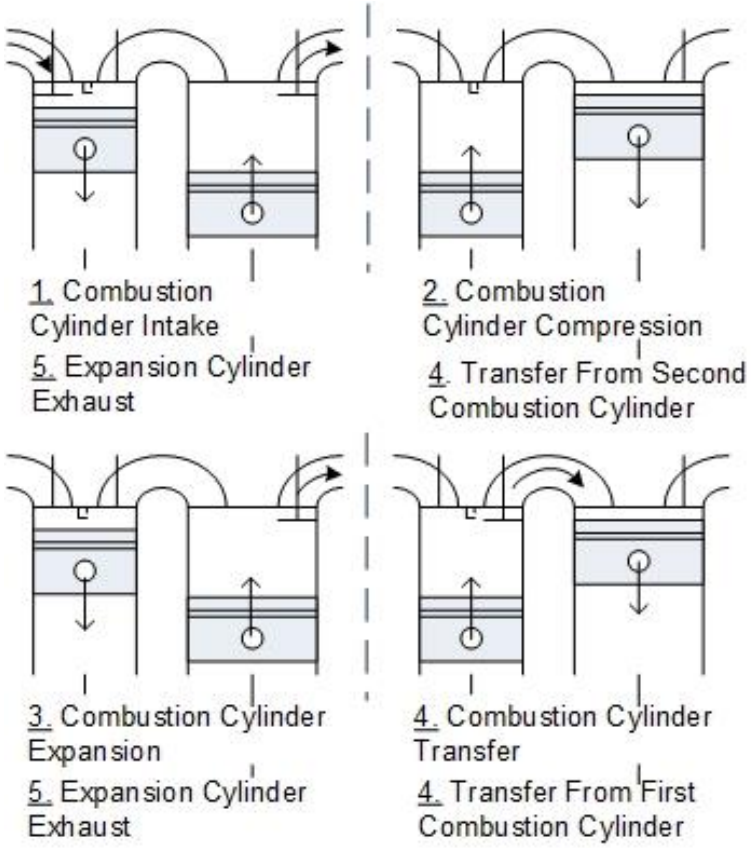

Figure 4. Stroke-by-stroke illustration of the 5-stroke engine process

2.2 Effective Geometric Expansion Ratio

The effective geometric expansion ratio (EGER) is defined as the ratio between the minimum compressed volume and the maximum expanded volume. Equation 5 is used to calculate EGER where V_{CCV} is the clearance volume of the combustion cylinder and V_{ECD} is the displacement volume of the expansion cylinder.

$$EGER = \frac{V_{CCV} + V_{ECD}}{V_{CCV}}$$

Equation 5: Effective Geometric Expansion Ratio

Equation 5 is only valid when the two cylinders are offset by 180 degrees. Under this condition, the displacement volume of the combustion cylinder can be ignored when calculating the EGER because the maximum expansion volume occurs when the expansion cylinder is at bottom dead center (BDC) resulting in the combustion cylinder being at top dead center (TDC). Therefore, the displaced volume is equal to zero and does not affect the EGER. The clearance volume of the expansion cylinder and transfer port volume are also ignored when calculating EGER as no work is performed during expansion into those volumes. However, transfer port geometry and expansion cylinder clearance volume still have an effect on the brake thermal efficiency of the 5-stroke engine because they play a role in the total pressure drop during the transfer process. The sensitivity of the 5-stroke to the transfer port volume and expansion cylinder clearance volume will be examined as part of the parametric study.

2.3 5-Stroke P-V Diagram

To examine the thermodynamics of the 5-stroke cycle, a composite P-V diagram with valve events and cycle classification labeled for both the combustion and expansion cylinder is shown in Figure 5. The expansion cylinder P-V diagram represents the total volume of the system, which is the sum of the expansion cylinder, combustion cylinder, and transfer port volumes. Starting at intake valve open (IVO) of the combustion cylinder, the intake process occurs until intake valve close (IVC). At IVC, the compression cycle begins in the combustion cylinder. After compression, combustion, and expansion have occurred in the combustion cylinder, the transfer valve opens (TVO)

connecting the combustion and expansion cylinders. For a brief portion of the cycle, an overlap exists between TVO in the combustion cylinder and exhaust valve close (EVC) in the expansion cylinder resulting in a brief portion of open cycle. The overlap between TVO and EVC serves the purpose of reducing the pressure rise in the expansion cylinder until closer to TDC of the expansion cylinder and allows the pressure in the combustion cylinder to start decreasing before BDC. If the EVC occurs earlier, the pressure in the expansion cylinder increases prematurely. Early EVC has two primary effects: first, expansion is reduced due to the increase in trapped mass in the expansion cylinder and, second pumping work in the expansion cylinder is increased due to an increase in trapped mass compression. The effect of the TVO, EVC overlap will be discussed further in the analysis portion. After EVC, the system is closed and the transfer process, or extended expansion occurs where additional work is performed by the expansion cylinder. As the expansion cylinder approaches BDC, exhaust valve open (EVO) occurs so that the remaining pressure can be released before IVO.

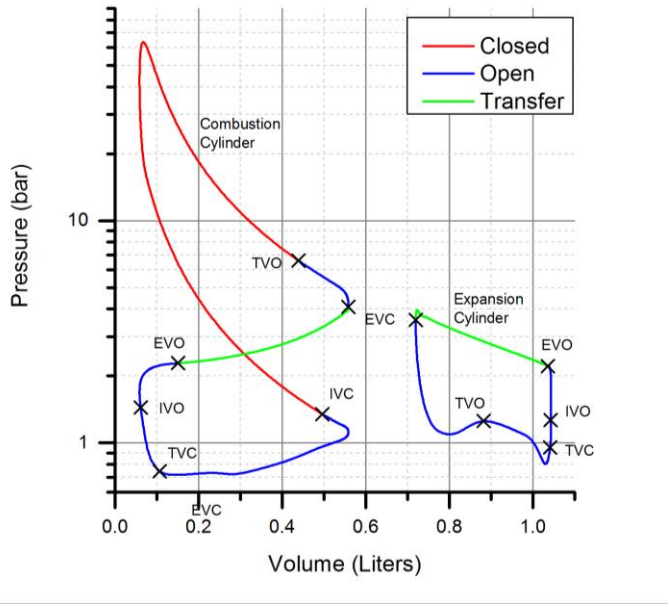

Figure 5. Detailed P-V diagram of center point 5-stroke cycle with valve event and cycle phases labeled

Optimally, EVO would occur at expansion cylinder BDC to maximize expansion work; unfortunately, it cannot be placed there due to pumping effects and increased IVO pressure. EVO timing effects on brake thermal efficiency will be discussed further in a later section. After a period where both the intake and exhaust valve are open, the transfer valve closes (TVC) separating the two cylinders. This allows the combustion cylinder to perform the intake stoke while the exhaust stroke occurs in the expansion cylinder. The overlap between IVO and TVC is similar to the overlap that occurs in the standard SI engine between the IVO and EVC. The total work produced by the 5-stroke is equal to the sum of the work loop in the combustion cylinder and the work loop of the expansion cylinder minus the work loop of the pumping curve. The combined P-V diagram will be used in this paper to visualize effects of parameters on 5-stroke engine efficiency.

3 Methods

3.1 Engine Model

To investigate the effects of various parameters on 5-stroke efficiency, a 1-D simulation was created using the GT Power® software. A two-cylinder standard SI engine was constructed for use as a reference model and to provide a starting point for development of the 5-stroke model. The initial bore, stroke, and CR were taken from a 2.0-liter GM engine used in cars such as the Chevrolet Malibu. Since physical testing was beyond the scope of the project the remaining parameters that could not be easily found online such as, parameters for friction, combustion, and valve lift and flow were taken from GT Power templates and remained constant for all configurations [27]. The Chen-Flynn friction model which calculates the friction mean effective pressure (FMEP) using 4 constants, the peak pressure in the cylinder, and the piston velocity was used to estimate the frictional losses of the engine [28].

$$FMEP = A + B * P_{max} + C * n + D * n^2$$

Equation 6: Chen-Flynn Friction Model

The SI-Weibe combustion model was used to model the combustion event. This model uses duration and exponent to determine the rate of energy release, and an anchor point that controls where 50% of the energy has been released for the fuel being used, in our model octane was the fuel used. The original valve lift profiles used in the standard SI engine model were modified using multipliers to change lift and duration during the

development of the 5-stroke model. A Design of Experiments (DOE) method was used to determine the center point valve lift, duration, and timing. In the DOE, the same multiplier was used for both lift and duration as well as during parameter sweeps.

A full intake system sub-model was required to improve accuracy. An intake system comprised of inlet ductwork leading to a side feed log style plenum connected to the intake port by straight runners was modeled to eliminate the loss of fuel through the inlet environment. Figure 3 shows the layout of the combustion cylinder, expansion cylinder, valve, and port configuration. The combustion cylinder consisted of a three-valve design with two intake, and one exhaust valve. Each combustion cylinder was connected to the expansion cylinder by a single transfer port that is open on the expansion cylinder side. The expansion cylinder consisted of a four-valve configuration but valves were only placed on the exhaust port. The expansion cylinder then was connected to an exhaust system through a modeled port into a single exhaust pipe.

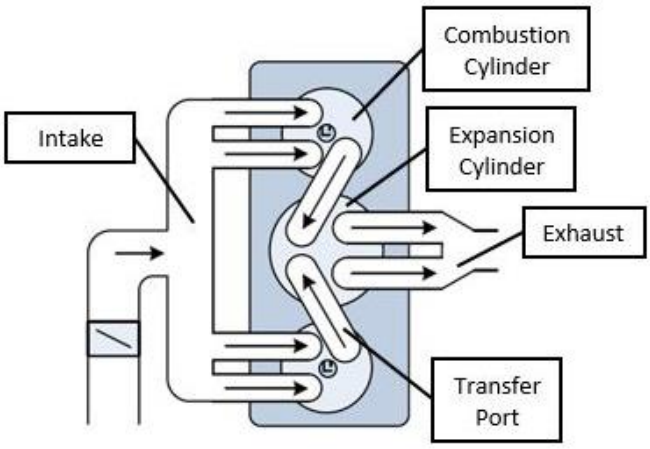

Figure 6. Cylinder arrangement with intake, transfer, and exhaust port layout

Parameter sweeps were conducted using the developed model by first establishing center-point values shown in Table 1. Chosen key parameters for examination included bore to

stroke ratio, EGER, transfer port length and exit diameter, expansion cylinder CR, cylinder offset, and intake, transfer, and exhaust valve lift profile multipliers, used to scale both lift and duration of the valve lift profiles. Sweeps were conducted by changing one parameter while others were held constant to examine the effects on engine efficiency.

	Cylinder		
	Combustion	Expansion	
Bore (mm)	86.00	101.59	
Stroke (mm)	86.00	101.59	
CR	9.5	12	
Offset (deg)	180		
	Valve		
	Intake	Transfer	Exhaust
Diameter (mm)	30	40	50
Multiplier	1.3	1.3	1.3
Duration (Lashed Lift) CAD	218.9	248.2	228.1
Max Lift (mm)	8.27	9.29	9.19
	Transfer Port		
Length (mm)	30.00		
Inlet Diameter (mm)	37.20		
Exit Diameter (mm)	48.38		

Table 1. Center point values for 5-stroke GT Power model

3.2 Vehicle Use

To examine the performance of the 5-stroke engine under normal driving conditions, the power required to maintain a constant speed was calculated using Equation 7. Dimensional values for a 2015 Chevrolet Malibu where used with the remaining values need to calculate the power requirement coming from the Bosch Automotive Handbook for a sedan and can be found in Table 2 [29], [30]**Error! Reference source not found.**. The GT Power® models for both the two-cylinder reference engine and 5-stroke were run at constant power output over a range of RPM's. This was done by implementing a throttle controller that adjusts the size of the throttle orifice to the required size for the given power output required at the RPM being examined. To examine the performance at various operating part-load points the power required at five different vehicle speeds (30, 40, 50, 60, and 70 mph) where determined to examine performance under typical driving conditions. This method was chosen over a theoretical load cycle because it provided a direct comparison of only the engines. If a theoretical load cycle is used a driveline system would be required since power output is a function of throttle position and RPM one of those variables would need to be constrained.

$$Pr = \left(Cr * Mv * G + \frac{1}{2} * \rho * C_d * A_v * S_v^2\right) * S_v$$

Equation 7: Power requirement for constant velocity

Weight (Mv)	1696 kg
Coefficient of rolling resistance (Cr)	0.013
Density of Air (ρ)	1.175 kg/m^3
Height	1.463 m
Width	1.854 m
Ride height	0.203 m
Frontal area (A_v)	2.336 m^2
Drag coefficient (C_d)	0.3

Table 2: Vehicle data for determining engine power requirement

Figure 7: 2015 Chevrolet Malibu

4 Results and Discussion

4.1 Baseline Model

The initial two-cylinder standard SI engine that the 5-stroke model was developed from served as a baseline for comparison. The two-cylinder model was initially run over a range of engine speed. Figure 8 shows that the maximum brake thermal efficiency was 29.32% and occurred at 3200 RPM and wide-open throttle. To minimize the effects of variables not included in the parametric study, the 5-stroke model used the maximum brake thermal efficiency operating point for all comparisons even though Figure 8 and 9

show improved 5-stroke performance at lower engine speed when compared to the 4-stroke.

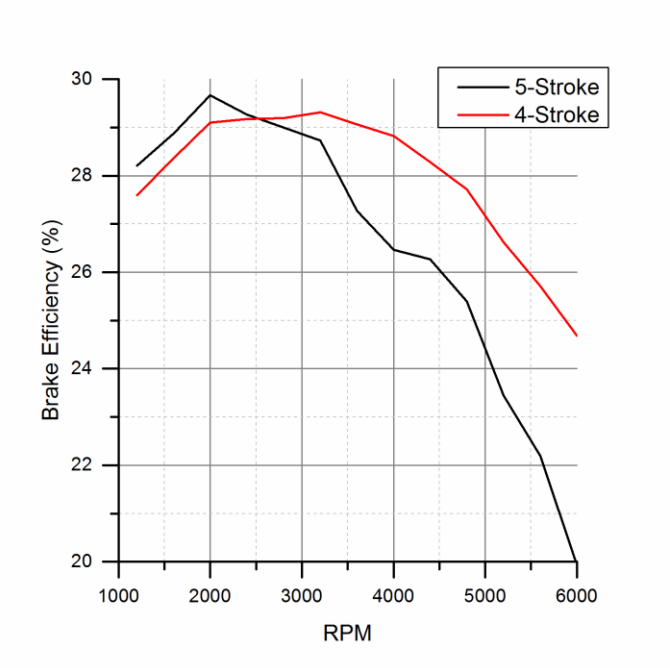

Figure 8. Brake efficiency vs RPM baseline 4-stroke model and 5-stroke models at WOT

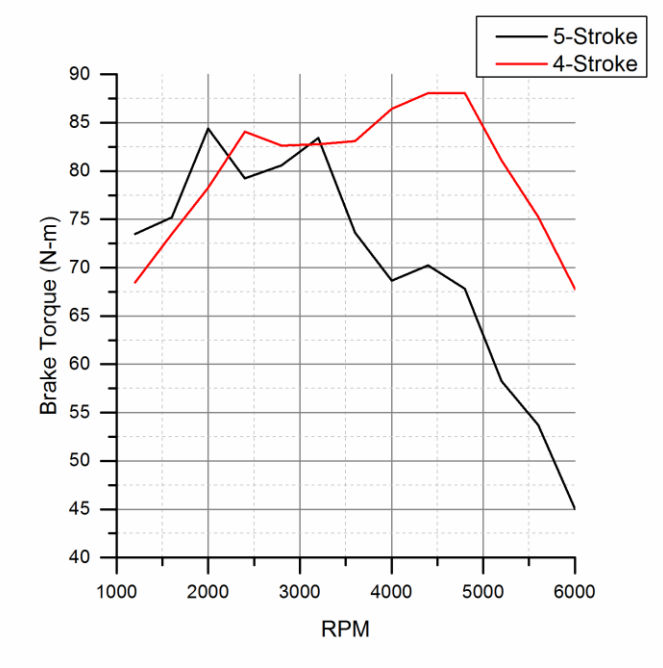

Figure 9. Brake torque vs RPM for baseline 4-stroke and 5-stroke models at WOT

4.2 Effective Geometric Expansion Ratio (EGER)

To examine the effect of EGER on the brake thermal efficiency of the 5-stroke cycle, a sweep of EGER values was conducted for three bore-to-stroke ratios. Three bore to stroke ratios of 0.6, 1, and 1.4 were selected to examine over EGER values from 10 to 20. Figure 10 shows the brake thermal efficiency percentage for the combined bore to stroke ratio and EGER at a given engine speed. As the bore to stroke ratio increases, the engine brake thermal efficiency increases for a given EGER. The primarily cause is from the reduction in estimated friction from the Chen-Flynn friction model. Since the constant terms in the Chen-Flynn model remain the same for all models, the reduction in piston velocity as the bore to stroke ratio increases, for the same EGER, results in a reduction in estimated friction. For higher EGER values, the brake thermal efficiency starts to decrease because for a given bore to stroke ratio, the mean piston velocity increases

resulting in increased friction as the EGER increases. The peak in brake thermal efficiency for each bore to stroke ratio represents the point where the increased work and friction from larger EGER are balanced.

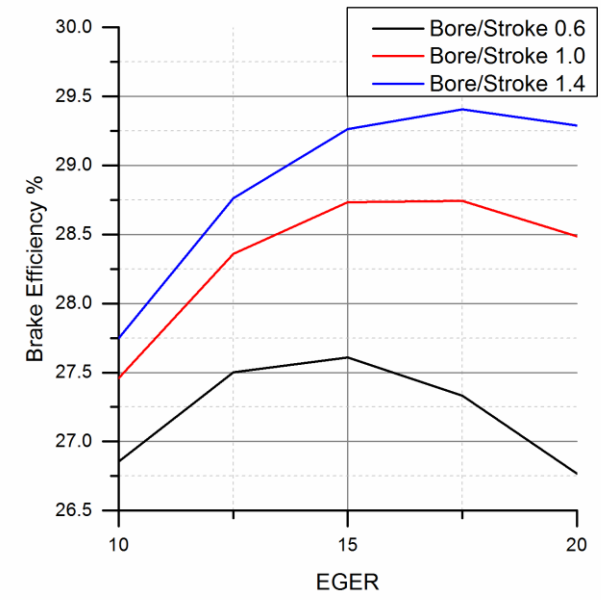

Figure 10. Brake efficiency vs EGER for expansion cylinder bore to stroke ratios of 5-stroke center point at 3200 RPM

The P-V diagram in Figure 11 shows that as EGER increases, the size of the combustion and expansion cylinder work loops increase and the combustion cylinder pumping loop decreases. The increase is the result of increased gas flowing from the combustion cylinder to the expansion cylinder during the transfer process. The increased transfer drives gains in brake thermal efficiency. As the EGER decreases, the maximum total volume occurs before the expansion cylinder reaches BDC. However, since EVO remains

constant the trapped mass is compression to the EGER value. The compression work along with the low EGER reduces indicated and brake thermal efficiency.

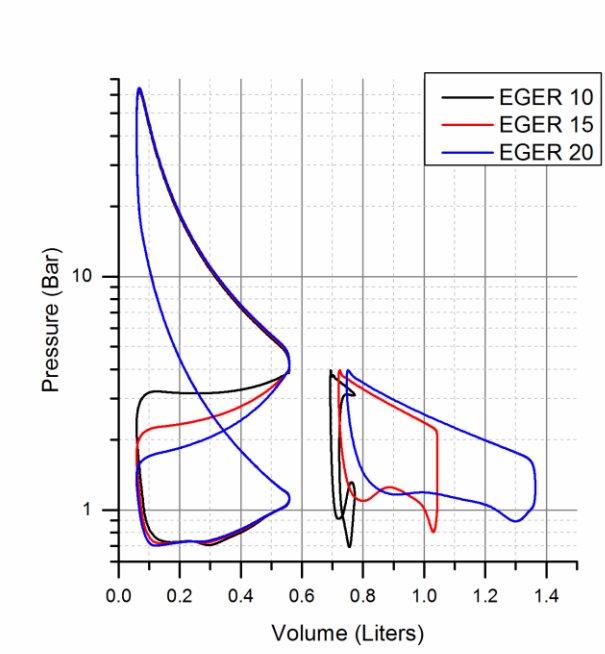

Figure 11. EGER P-V diagram comparison at 3200 RPM and bore to stroke ratio of 1

4.3 Transfer Port Volume

When calculating the EGER, the transfer port and expansion cylinder clearance volume are ignored because work is not performed during expansion into dead space volumes. To determine the effect that the dead space volume and shape have on the 5-stroke cycle, the length and exit diameter of the transfer port were varied. The transfer port length ranged from 10-50 mm with exit diameters ranging from 1 to 1.6 times the transfer port inlet diameter. Figure 12 shows that as the length of the transfer port increases, there is a reduction in brake thermal efficiency, but by increasing the transfer port length from 10-50 mm the change in efficiency is only 0.25%. The maximum brake thermal efficiency occurs when the exit diameter is 1.1-1.2 times the transfer port inlet diameter. By

increasing the exit diameter, the transfer port becomes a diffuser that reduces pressure losses during the transfer between the combustion and expansion cylinder. The maximum brake thermal efficiency values represent the points where the pressure drop reduction from a diffuser is surpassed by the pressure loss due to increased volume.

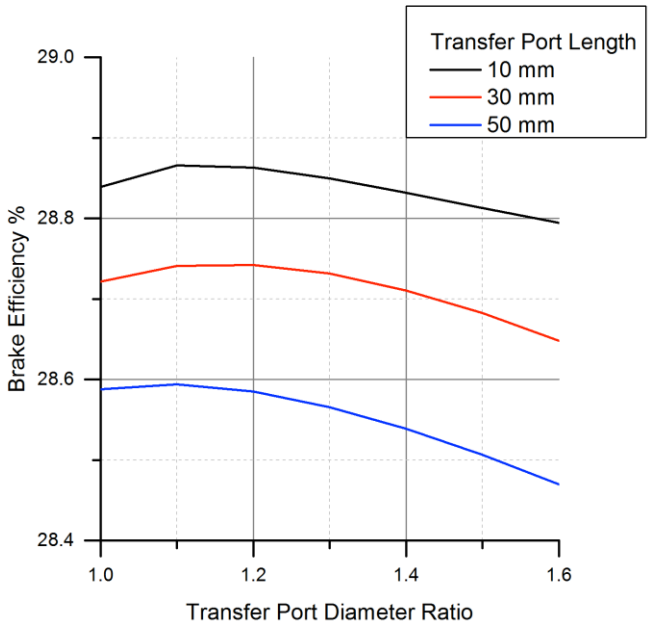

Figure 12. Brake efficiency vs transfer port exit diameter ratio for multiple port lengths at 3200 RPM

The P-V plot in Figure 13 shows that as the transfer port length increases, the expansion cylinder work loop shifts to the right. Since the EGER remains constant, the volume delta of the expansion cylinder work loop remains the same. As the expansion cylinder work loop moves to the right the peak pressure in the expansion cylinder decreases as the result of increased pressure losses from increased dead volume. The reduction in pressure reduces the expansion cylinder work loop area. The reduced peak expansion cylinder

pressure decreases the pressure in the combustion cylinder during the transfer stroke. This increases the combustion cylinder work loop and decreases the pumping loop. The offset from gains in increased expansion cylinder loop area and losses in decreased combustion cylinder work and increased pumping loop results in minimal changes in brake thermal efficiency for changes in transfer port length.

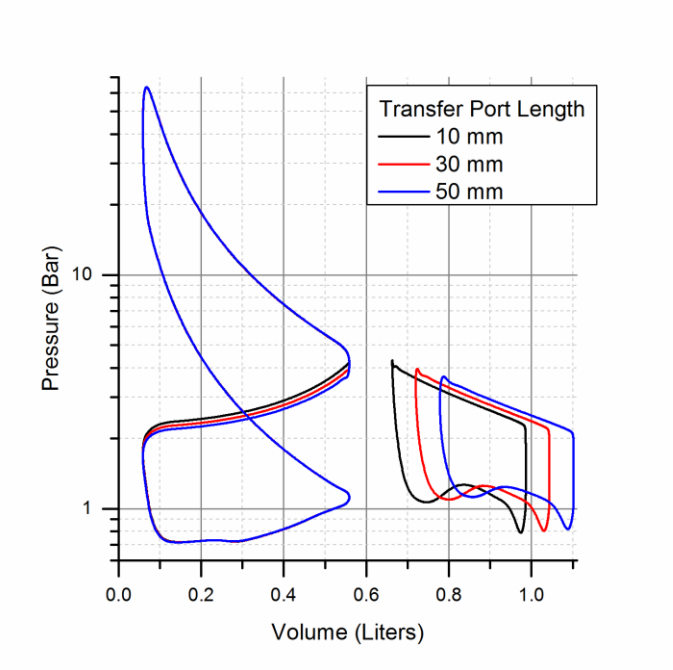

Figure 13. Transfer port length P-V diagram comparison at 3200 RPM with transfer port diameter ratio of 1.3

To examine the effect that expansion cylinder clearance volume has on the 5-stroke the expansion cylinder CR was varied from 10-20 for all three bore to stroke ratios with an EGER of 15. Figure 14 shows that for all three bore to stroke ratios the break efficiency increased as the expansion cylinder CR increased. The increase in brake thermal efficiency is the result of reduced pressure loss from dead space expansion leading to

higher peak expansion cylinder pressure. The change in brake thermal efficiency ranges from 0.084%-0.104% for the expansion cylinder CR's and bore to stroke ratios evaluated. The results indicate that changing expansion cylinder CR has a minimal effect on 5-stroke performance.

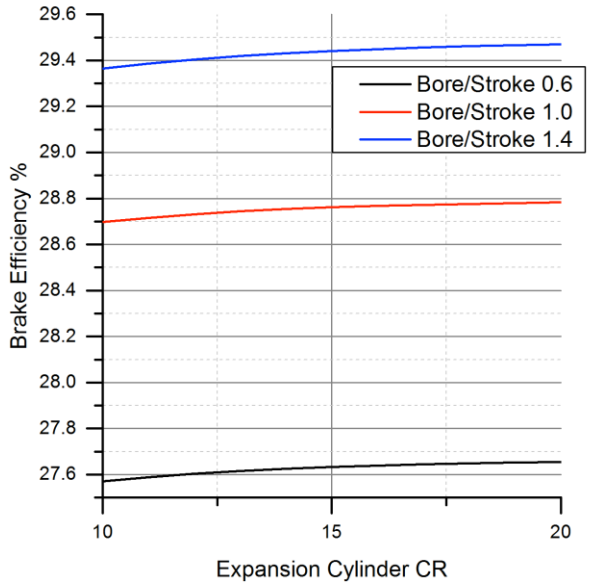

Figure 14. Brake efficiency vs expansion cylinder CR at 3200 RPM for various bore to stroke ratios with EGER of 15

4.4 Valve Lift Profile Multipliers (VLPM)

Since the 5-stroke relies on three separate valve lift profiles (VLPs) instead of two for a conventional SI engine, center-point VLPs were modified individually using a single multiplier controlling both lift and duration. The lift and duration multiplier ranged from 1-1.6 for the three different VLPs. Figure 15 shows that the maximum brake thermal efficiency occurs when the intake and transfer valve lift profile multiplier (VLPM) is 1.3

with the exhaust maximum occurring when the VLPM is between 1.4 and 1.5. Of the three VLPs, the transfer VLPM change has the largest effect on the brake thermal efficiency when compared to the intake and exhaust VLPM's. The following sub sections thoroughly examine the effects of each valve and VLPM.

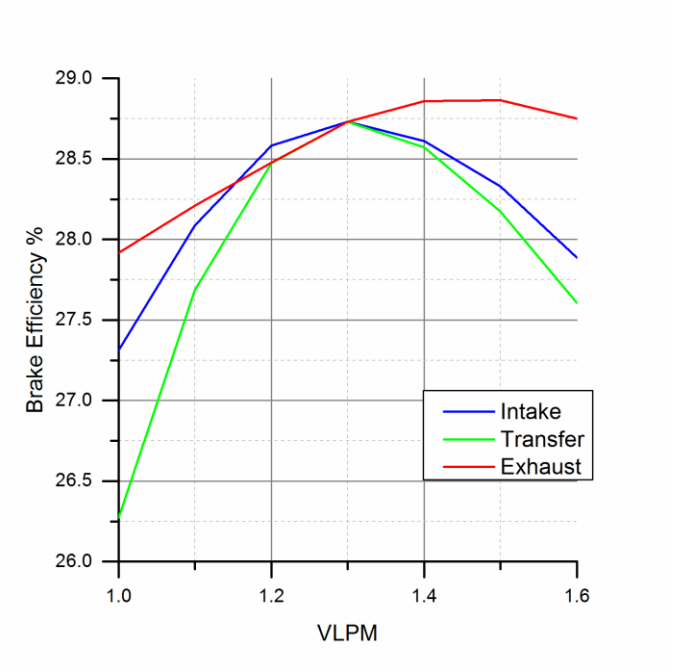

Figure 15. Brake efficiency vs VLPM for intake, transfer, and exhaust valve at 3200 RPM

4.5 Intake VLPM

Changing the intake VLP varied the brake thermal efficiency from 27.3% to 28.4% over the range of VLPM's examined. Figure 16 shows that as IVO is delayed, when the intake VLPM is 1, a large dip in pressure during the intake stroke appears. This dip significantly increases the area of the combustion cylinder pumping loop. The larger dip is the result of IVO occurring after TVC occurs and the combustion cylinder being on the down stroke.

The advancement of IVO results in a larger overlap between the intake, transfer, and exhaust valve as seen in Figure 17. Increasing overlap by advancing IVO results in increased residual exhaust gas flow into the intake manifold. This is caused by the decrease in time between EVO and IVO, which reduces exhaust blow-down resulting in higher cylinder pressure at IVO. As IVC is advanced there is a decrease in trapped mass in the combustion cylinder, which leads to lower peak cylinder pressure. The reduction in peak combustion cylinder pressure causes a reduction in pressure throughout the entire cycle. Delaying IVC, when the intake VLPM is 1.6, also results in a reduction in trapped mass leading to the reduction in peak pressure. The reduction in trapped mass has the same effect as reducing the EGER, which leads to the reduction in brake thermal efficiency. Delaying IVO increases the pumping work in the combustion cylinder leading to a reduction in brake thermal efficiency.

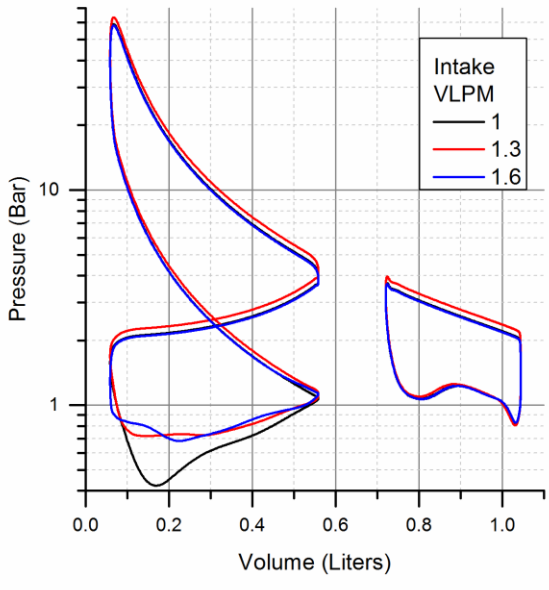

Figure 16. Intake VLPM P-V diagram comparison at 3200 RPM

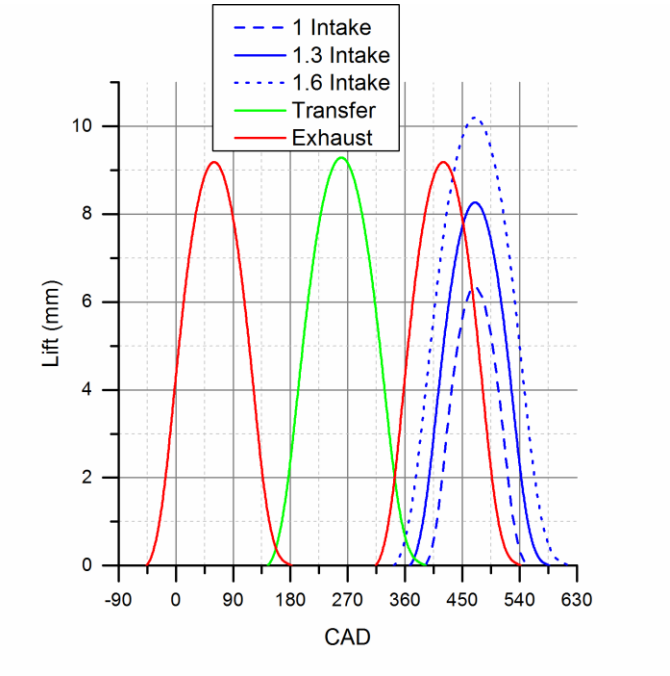

Figure 17. 5-stroke VLP with intake VLPM profiles

4.6 Transfer VLPM

The transfer VLP in the 5-stroke controls the transfer process between the combustion and expansion cylinders. With the brake thermal efficiency ranging from 26.5% to 28.4% for the VLPM's examined, the transfer VLP has the largest impact on the performance of the 5-stroke compared to the intake and exhaust valve. Figure 18 shows that as TVO was delayed for a transfer VLPM of 1, the peak pressure in the expansion cylinder decreased. The decrease in peak pressure is the result of the expansion cylinder being further past TDC, resulting in increased dead space volume at the beginning of the transfer process. As the transfer process is delayed past TDC of the expansion cylinder, the amount of expansion work before EVO decreases. For a transfer VLPM of 1.6, the P-V diagram shows that as TVO is advanced, the pressure rise in the expansion cylinder is advanced. This causes the peak pressure in the expansion cylinder to be advanced before TDC and

the pressure drop in the combustion cylinder to advance. The advancement of peak cylinder pressure creates a small pumping loop in the expansion cylinder. Figure 19 shows that by advancing TVO, the overlap between the transfer and exhaust valve increases. Increasing overlap results in increased blow-by of exhaust gas past the exhaust valve before EVC and expansion. This reduces the pressure in the expansion cylinder during the expansion process. The advanced pressure rise creates a pumping loop in the expansion cylinder, advanced pressure drop in the combustion cylinder, and increased exhaust blow-by during overlap thus reducing in brake thermal efficiency. Figure 18 shows a large pressure spike in the combustion cylinder near the end of the transfer process for a transfer VLPM of 1. The spike is caused by advancing TVC before the combustion cylinder piston reaches TDC. If TVC occurs before TDC of the combustion cylinder, trapped exhaust gas is recompressed resulting in increased pressure at IVO causing exhaust gas to flow into the intake. The presence of exhaust gas in the intake decreases the amount of fresh air and fuel that enters the cylinder which reduces peak combustion cylinder pressure similar to advancing IVO. The recompression spike increases the combustion cylinder pumping loop and reduces peak pressure, decreasing brake thermal efficiency.

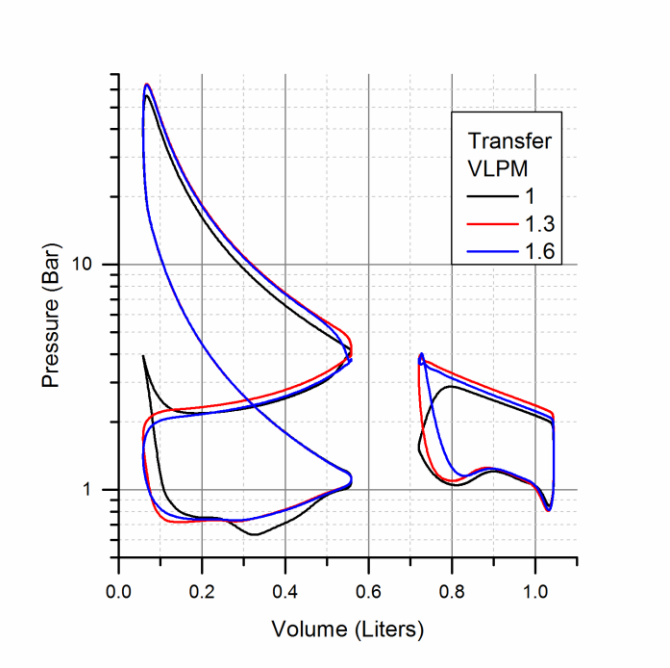

Figure 18. Transfer VLPM P-V diagram comparison at 3200 RPM

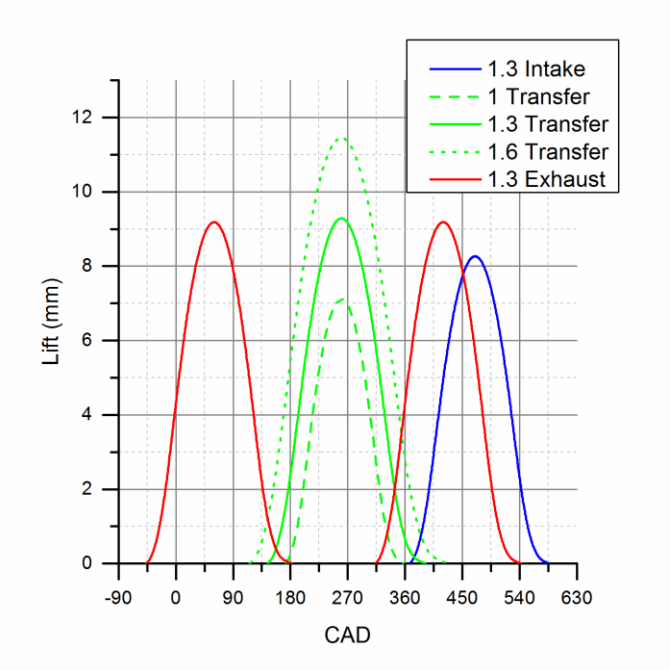

Figure 19. 5-stroke VLP with transfer VLPM profiles

4.7 Exhaust VLPM

Figure 15 shows that the exhaust VLPM has the smallest impact on brake thermal efficiency compared to the intake and transfer valve, with efficiencies ranging from 27.8% to 28.7%. Figure 20 shows as EVO is delayed the pressure at IVO increases resulting in exhaust gas flowing into the intake. The increased pressure produces a larger pumping loop in the combustion cylinder. Figure 21 shows that this is because as EVO is delayed, the time for blow-down of exhaust gas before the IVO is decreased. As EVO is advanced, the blow-down process in the expansion cylinder is advanced. This results in decreased pumping work in the combustion cylinder as EVO is advanced. Figure 20 shows that as EVC is advanced, when the exhaust VLPM is 1, the pressure rise in the expansion cylinder is advanced. The trapped mass in the expansion cylinder increases as EVC is advanced, reducing the mass transfer between the combustion and expansion cylinders. By delaying EVC, Figure 20 shows that the pressure rise in the expansion cylinder is delayed. This reduces the trapped mass in the expansion cylinder resulting in reduced pressure during the expansion process. Figure 21 shows that as EVC is delayed, the overlap between TVO and EVC increases. This increases exhaust blow-by further reducing the trapped mass. As the exhaust VLPM increases the time that the exhaust valve is closed reduces the amount of expansion work generated by the expansion cylinder. Figure 15 shows that the peak brake thermal efficiency occurs between an exhaust VLPM's of 1.4 and 1.5 where the tradeoff between reduced expansion work and pressure rise reaches a maximum.

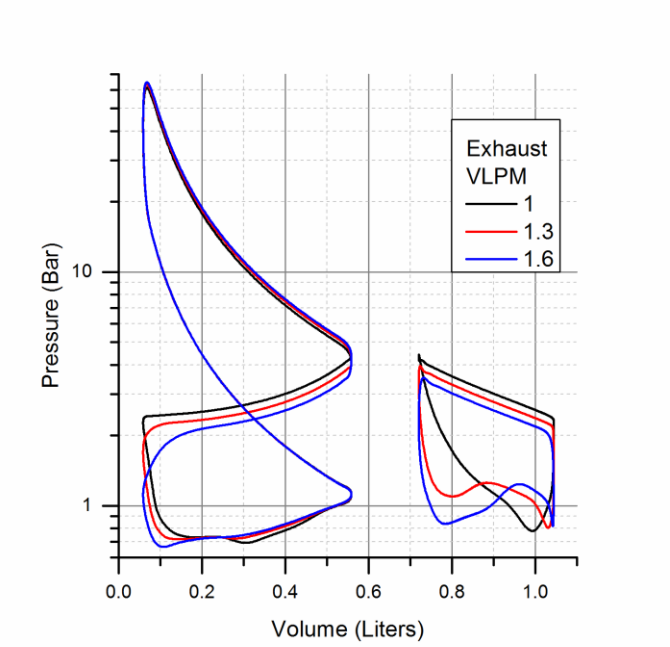

Figure 20. Exhaust VLPM P-V diagram comparison at 3200 RPM

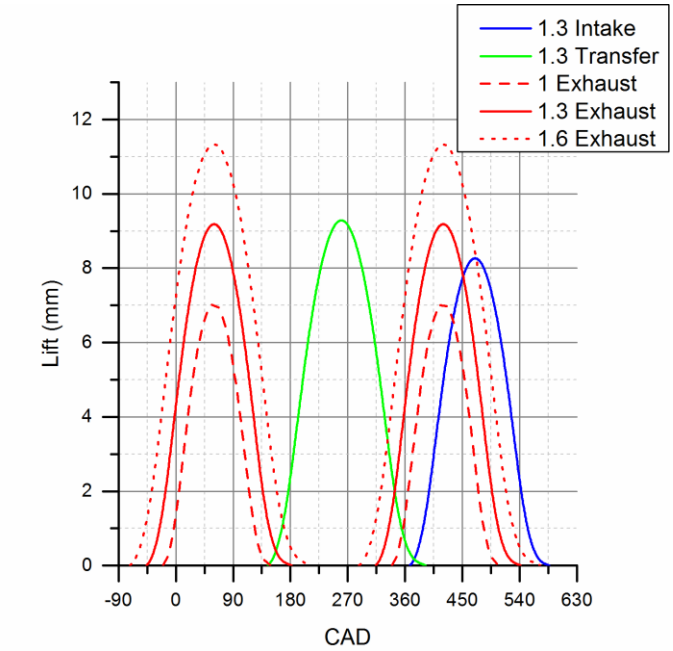

Figure 21. 5-stroke VLP with exhaust VLPM profiles

4.8 Cylinder Angle Offset

Ailloud et al. discussed the benefits of offsetting the expansion cylinder from the combustion cylinders to improve valve train packaging, transfer port layout, and synchronizing cycles between the combustion and expansion cylinder. Figure 22 shows that offsetting the expansion cylinder from the combustion cylinder effects EGER and CAD where maximum expansion occurs. When the combustion and expansion cylinders are offset by 165 or 195 degrees the maximum EGER increases to 15.91 and occurs 61 degrees before or after the combustion cylinder reaches TDC.

Maintaining the same transfer valve timing with respect to the combustion cylinder and exhaust valve timing with respect to the expansion cylinder, changing cylinder offset has multiple effects. When the offset is decreased, below 180 degrees, the overlap between TVO and EVC is also decreased which reduces exhaust blow-through. EVO is also advanced with respect to the combustion cylinder reducing combustion cylinder pressure at IVO. Figure 23 shows that the expansion process is advanced with respect to combustion cylinder resulting in lower pressures in the combustion cylinder during the transfer process. This increases the work loop and decreases the pumping loop in the combustion cylinder. Since the expansion cylinder is closer to TDC at TVO, decreasing the offset reduces expansion cylinder pumping work. All of this combines for improved brake thermal efficiency as the offset between cylinders is decreased as seen in Figure 24.

The same is not true as the offset is increased beyond 180 degrees. As Figure 22 shows the maximum EGER occurs after the expansion cylinder has reached TDC. Increased offset, above 180 degrees, increases overlap between TVO and EVC. Increased

cylinder offset also delays the transfer process between the combustion and expansion cylinder leading to increased pressure in the combustion cylinder and decreased pressure in the expansion cylinder. Since TVO is advanced with respect to the expansion cylinder the pressure rises prematurely in the expansion cylinder. The combination of the premature pressure rise from advanced TVO and the minimum total volume occurring after EVO results in recompression. This causes a pumping loop to form on the expansion cylinder P-V diagram as seen in Figure 23. Increased offset causes higher combustion cylinder pressure at IVO do to the delay of EVO with respect to the combustion cylinder resulting in increased exhaust blow-back into the intake. All of this leads to an increased combustion cylinder pumping loop and a reduction in both the combustion and expansion cylinder work loops. Figure 24 shows that as the offset between the combustion and expansion cylinder increases the brake thermal efficiency decreases.

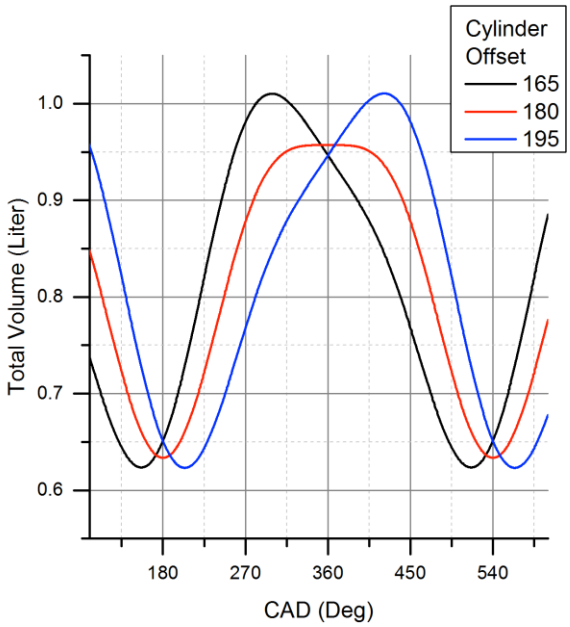

Figure 22. Combined volume of combustion and expansion cylinder versus CAD for EGER of 15 and bore to stroke ratio of 1 for various cylinder offsets

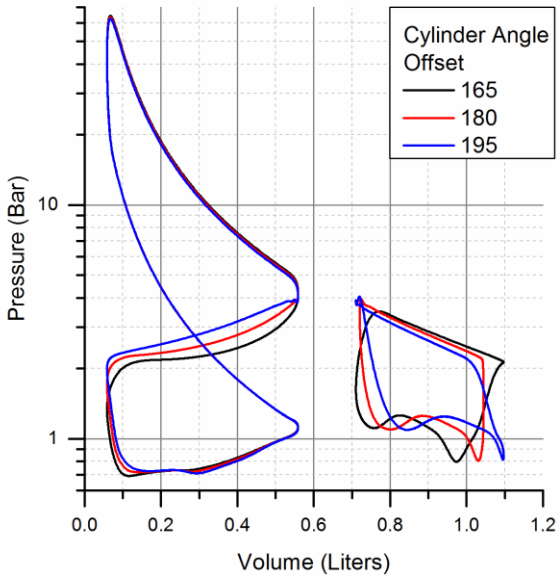

Figure 23. Cylinder offset P-V diagram comparison at 3200 RPM, EGER of 15, and bore to stroke ratio of 1

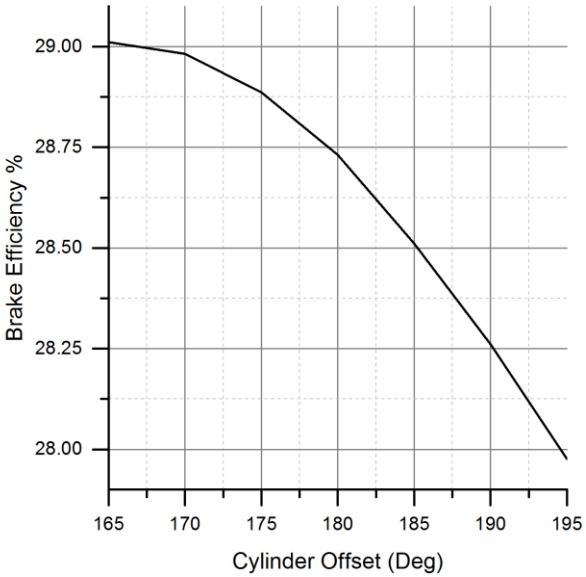

Figure 24. Brake efficiency vs cylinder offset at 3200 RPM, EGER of 15, and bore to stroke ratio of 1

4.9 Vehicle Application Comparison

While WOT conditions are useful for comparing the peak performance of an engine in a passenger vehicle, practical engines operate at this mode only occasionally. In this section, indicated thermal efficiency, defined as the ratio of the thermodynamic work performed by the cycle to the amount of fuel energy added to the system, is examined for part-load operation. Figure 25 shows that the indicated thermal efficiency decreases as engine speed increases for higher vehicle speeds but levels off more at lower speeds. As expected, the 5-stroke model shows improved indicated thermal efficiency over the 4-stroke model for all vehicle speeds examined. The increase in indicated efficiency is the result of additional work being performed by the expansion cylinder. This shows that from an indicated (thermodynamic) standpoint, the 5-stroke engine results in increased work compared to the 4-stroke engine.

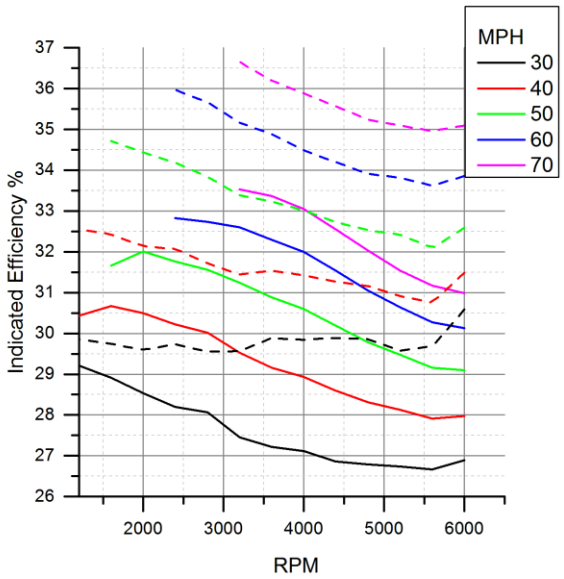

Figure 25: Indicated thermal efficiency comparison of 4 and 5-stroke at five vehicle speeds (i.e. constant engine power). Solid lines represent 4-stroke, dashed lines represent 5-stroke

While indicated thermal efficiency provides insight on the total work performed by the engine cycle, brake thermal efficiency is a better measure of the efficiency of an actual engine because it represents the ratio of the useable shaft power produced by the engine for a given amount of fuel. Figure 26 shows the widening gap in brake efficiency between a 4-stroke and a 5-stroke engine as engine speed increases. The reduction in brake thermal efficiency as engine speed increases is expected as the torque decreases and the friction increases due to higher piston velocity. The reason that the 4-stroke out performs the 5-stroke in terms of brake thermal efficiency is due to a difference in friction loss. In a 5-stroke engine, the additional cylinder increases friction, which is magnified by an increase in piston velocity as engine speed increases.

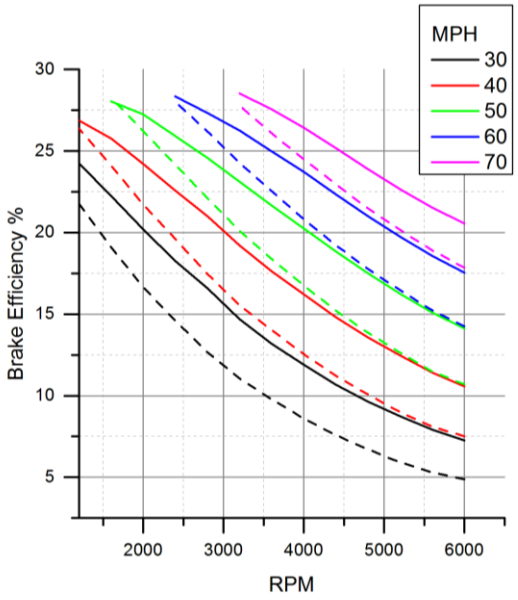

Figure 26: Brake thermal efficiency comparison of 4 and 5-stroke engines at five vehicle speeds (i.e. constant engine power). Solid lines represent 4-Stroke, dashed lines represent 5-stroke

5 Summary/Conclusions

A 1-D simulation in GT Power was used to conduct a parametric study on how various parameters affect the performance of a 5-stroke SI engine. A three cylinder 5-stroke model was developed from a two cylinder 4-stroke model that served as the base line comparison. The wide-open throttle point provides peak brake thermal efficiency for the 4-stroke model was used for all parameter sweeps. Of the parameters investigated, the bore to stroke ratio, EGER, transfer VLPM, and cylinder offset had the most significant impact on the brake thermal efficiency of the 5-stroke engine. At the operating point examined in the work, no individual parameter change resulted in the 5-stoke brake

thermal efficiency being higher than the 4-stroke model. The center point 5-stroke model has a maximum increase in brake thermal efficiency of 0.57% over the 4-stroke model at lower engine speed. This slight efficiency increase does not translate to full vehicle operation where throttling and frictional effects significantly reduce the brake thermal efficiency of the 5-stroke engine compared to the 4-stroke.

While further work could be performed to investigate more complex interactions between operating parameters to achieve higher efficiency gains, the results of this study indicate that the 5-stroke concept as modeled is not a viable solution for significantly increasing efficiency compared to the base 4-stroke engine. This work revealed that the 5-stroke engine suffers mainly due to increased friction of the additional cylinder that overwhelms advantages of additional expansion work. Further breakthroughs in friction reduction and in novel thermodynamic cycles that yield more work from the expansion cylinder may offer a pathway to higher efficiency from such engine concepts.

References

[1] US. EPA, "EPA and NHTSA Set Standards to Reduce Greenhouse Gases and Improve Fuel Economy for Model Years 2017-2025 Cars and Light Trucks," 2012.

[2] M. L. Poulton, *Alternative Engines for Road Vehilces*. Computational Mechanics Publications, 1994.

[3] N. A. Otto, "Improvement in gas-motor engines," United States Patent 194047, 1877.

[4] J. J. G. Martins, K. Uzuneanu, B. Ribeiro, and O. Jasasky, "Thermodynamic Analysis of an Over-Expanded Engine," *SAE Tech. Pap.*, no. 2004–01–0617, 2004.

[5] J. M. Mallikarjuna and V. Ganesan, "Theoretical and Experimental Investigations of Extended Expansion Concept for SI Engines Reprinted From : Engine Modeling Techniques : SI and Diesel," *SAE Tech. Pap.*, no. 2002–01–1740, 2002.

[6] J. M. Mallikarjuna and V. Ganesan, "Numerical Predictions and Experimental Investigations on Extended Expansion Engine Performance and Exhaust Emissions," *SAE Tech. Pap.*, no. 2000–01–1415, 2000.

[7] P. Ferrey, Y. Miehe, C. Constensou, and V. Collee, "Potential of a variable compression ratio Gasoline SI engine with very high expansion ratio and variable valve actuation," *SAE Tech. Pap.*, no. 2014–01–1201, 2014.

[8] Y. Sakata, K. Yamana, K. Nishida, T. Shimuzu, S. Shiga, M. Araki, H. Nakamura, and T. Obokata, "A Study on Optimization of an Over-Expansion Cycle Gasoline Engine with Late-Closing of Intake Valves," *SAE Tech. Pap.*, no. 2007–24–0089, 2007.

[9] M. K. Anderson, D. N. Assanis, and Z. S. Filipi, "First and Second Law Analyses of a Naturally-Aspirated, Miller Cycle, SI Engine with Late Intake Valve Closure," *SAE Tech. Pap.*, no. 980889, 1998.

[10] R. Miller, "Supercharged Engine," United States Patent 2817322, 1957.

[11] Y. Wan and A. Du, "Reducing part load pumping loss and improving thermal efficiency through high compression ratio over-expanded cycle," *SAE Tech. Pap.*, pp. 2013–01–1744, 2013.

[12] G. Vent, C. Enderle, N. Merdes, F. Kreitmann, and R. Weller, "The New 2 .0l Turbo Engine from the Mercedes- Benz 4-Cylinder Engine Family," *2nd Aachen Colloq. China*, 2012.

[13] O. M. FRANÇA JUNIOR, "Impact of the Miller Cycle in the Efficiency of an Fvvt (Fully Variable Valve Train) Engine," *SAE Tech. Pap.*, no. 2009–36–0081, 2009.

[14] C. Wang, R. Daniel, and H. Xu, "Research of the Atkinson Cycle in the Spark Ignition Engine," *SAE Tech. Pap. Pap.*, no. 2012–01–0390, 2012.

[15] P. Pertl, A. Trattner, A. Abis, S. Schmidt, R. Kirchberger, and T. Sato, "Expansion to Higher Efficiency - Investigations of the Atkinson Cycle in Small Combustion Engines," *SAE Tech. Pap.*, no. 2012–32–0059, 2012.

[16] J. A. C. Kentfield, "Extended , and Variable , Stroke Reciprocating," *SAE Tech. Pap.*, no. 2002–01–1941, 2002.

[17] A. Boretti and J. Scalzo, “Exploring the Advantages of Variable Compression Ratio in Internal Combustion Engines by Using Engine Performance Simulations,” *SAE Tech. Pap.*, no. 2011–01–0364, 2011.
[18] S. Watanabe, H. Koga, and S. Kono, “Research on Extended Expansion General-Purpose Engine Theoretical Analysis of Multiple Linkage System and Improvement of Thermal Efficiency,” *SAE Tech. Pap.*, no. 2006–32–0101, 2006.
[19] P. Aug, “Gas Engine,” United States Patent 367496, 1887.
[20] L. Miklanek, V. Klir, O. Vitek, and O. Gotfryd, “Study of Unconventional Cycles (Atkinson and Miller) with Mixture Heating as a Means for the Fuel Economy Improvement of a Throttled SI Engine at Part Load,” *SAE Tech. Pap.*, no. 2012–01–1678, 2012.
[21] J. Taylor, N. Fraser, R. Dingelstadt, and H. Hoffmann, “Benefits of late inlet valve timing strategies afforded through the use of intake Cam-In-Cam applied to a gasoline turbocharged downsized engine,” *SAE Tech. Pap.*, no. 2011–01–0360, 2011.
[22] C. J. Scuderi, “Split Four Stroke Cycle Internal Combustion Engine,” United States Patent 6543225, 2003.
[23] F. Phillips, I. Gilbert, J.-P. Pirault, and M. Megel, “Scuderi Split Cycle Research Engine: Overview, Architecture and Operation,” *SAE Tech. Pap.*, no. 2011–01–0403, 2011.
[24] D. Branyon and D. Simpson, “Miller cycle application to the Scuderi split cycle engine (by downsizing the compressor cylinder),” *SAE Tech. Pap.*, vol. c, no. 2012–01–04, 2012.
[25] G. Schmitz, “Five Stroke Internal Combustion Engine,” United States Patent 6553977, 2003.
[26] C. Ailloud, B. Delaporte, G. Schmitz, A. Keromnes, and L. Le Moyne, “Development and Validation of a Fife Stroke Engine,” *SAE Tech. Pap.*, no. 2013–24–0095, 2013.
[27] G. T. Inc., “GT-Power User’s Manual and Tutorial GT-Suite TM Version 7.4.” 2013.
[28] S. Chen and P. Flynn, “Development of a Single Cylinder Compression Ignition Research Engine,” *SAE Tech. Pap.*, no. 650733, 1965.
[29] “2015 Malibu Model & Specs,” 2015. [Online]. Available: http://www.chevrolet.com/2015-malibu-mid-size-sedan/specs/trims.html?ppc=MICROSOFT_700000001299233_71700000013688493_58700001099197904_p9960935498&gclid=CJjcyq_f-ssCFQhOMgodIowJkQ&gclsrc=ds#.
[30] R. Bosch, *BOSCH Automotive Handbook*, 8th ed. Wiley, 2011.